

Title: Geological evidences of surface rupture related to a 17th century destructive earthquake in Betic Cordillera (SE Spain): constraining the seismic hazard of the Alhama de Murcia Fault

Authors: José J. Martínez-Díaz^{*}; Jorge Alonso-Henar; Juan M. Insua-Arévalo; Carolina Canora; Julian García-Mayordomo; Emilio Rodríguez-Escudero; José. A. Álvarez-Gómez; Marta Ferrater; María Ortuño; Eulalia Masana.

Full mailing address for each author

José J. Martínez-Díaz; José. A. Álvarez-Gómez; Jorge Alonso-Henar and
Juan M. Insua-Arévalo:

TecTact Group, Departamento de Geodinámica, Estratigrafía y Paleontología
Universidad Complutense de Madrid
C/ Jose A. Novais 12, 28040 Madrid, Spain

Carolina Canora; Emilio Rodríguez-Escudero:
Dept. Geología y Geoquímica, Facultad de Ciencias,
Universidad Autónoma de Madrid, C/ Francisco Tomás y Valiente, 7, 28049 Madrid, Spain

Julian García Mayordomo:
Instituto Geológico y Minero de España, C/ Calera, 1, Tres Cantos, 28760 Madrid, Spain

Marta Ferrater, María Ortuño; Eulalia Masana:
Risnat group and Geomodel institute. Departament de Dinàmica de la Terra i l'Oceà Universitat de
Barcelona

^{*}Corresponding author address: Departamento de Geodinámica, Estratigrafía y Paleontología,
Universidad Complutense de Madrid. C/ Jose A. Novais, 12
28040 Madrid, Spain. ORCID: 0000-0003-4846-0279

Abstract

Constraining the date of the last major event occurred in a fault is of paramount importance in probabilistic seismic hazard assessment when time-dependent models are considered. Eight of the twelve destructive earthquakes occurred in the eastern Betic Cordillera since 16th century, are located less than 10 km away from the Alhama de Murcia fault (AMF). Up to now, it has not been identified any geological evidence on the ground surface to associate these events with the activity of specific fault sections of the AMF. In this work we present the first geological evidence of the catastrophic 1674 event occurred at Lorca (SE Spain). The excavations carried out at La Torrecilla creek exposed archaeological remains from the Arab period affected by 55 ± 20 cm offset by the AMF fault. This event reached intensity VIII and produced 30 fatalities at Lorca for an estimated population of 7300 inhabitants. This supports the occurrence of earthquakes with surface rupture in the historical epoch on the Alhama de Murcia Fault and reinforces the results obtained in previous paleoseismological work. The theoretical scenarios of maximum magnitudes and recurrence time obtained by combining this historical event with the fault slip rate allow us to conclude that the seismic hazard associated with maximum magnitude events in this section could be high. In addition, the static Coulomb stress transferred to the Góñar-Lorca section by the 2011 (Mw 5.2) Lorca earthquake may have significantly increased the hazard.

Key words: Surface rupture, active fault, seismic hazard, Betic Cordillera, Alhama de Murcia Fault.

Acknowledgments

This research was funded by the Secretaria de Estado de Investigación, Desarrollo e Investigación (MINECO) project INTERGEO (CGL2013-47412-C2-1-P). We thank Raquel Martín (IGME), Stella Moreiras (Conicet, Argentina) and Octavi Gómez, Roberto Escudero y Albert Baguer (Barcelona University), for their support in the field work and Agustín Sánchez Sánchez from AIA Estudio for his support with the topographic data acquisition.

1 Introduction

The Eastern Betic Cordillera, southeast of the Iberian peninsula, shows a low to moderate instrumental seismicity with earthquakes of magnitude $M_w < 5.5$. (e.g., [García-Mayordomo et al., 2007](#); [Rodríguez-Escudero et al., 2013](#)). During the last 50 years, the maximum recorded magnitude has been $M_w 5.2$ during the Lorca 2011 seismic crisis ([Lopez-Comino et al., 2011](#)). Within this time window another five seismic series produced significant damage (Lorca 1977, $M_w 4.2$; Adra 1993-1994, $M_w 5.0$; Bullas 2002, $M_w 5.0$; La Peca 2005, $M_w 4.8$). According to the Spanish Seismic Catalogue ([IGN, 2017, see Data and Resources](#)), the intensity values of these events did not exceed VII (EMS98). Most of these earthquakes have been interpreted as a result of the activity of small faults located in the crustal blocks bounded by the large NE-SW strike slip faults that cross the region ([García-Mayordomo, 2005](#); [Rodríguez-Escudero et al., 2013](#)) with the exception of the Lorca earthquakes that are associated with the activity of short sections of the Alhama de Murcia Fault (AMF) ([Martínez-Díaz et al., 2012b](#)).

In spite of the low damaging seismic activity occurred during the last century, the historical seismic catalogue shows that at least 12 destructive earthquakes with intensity $EMS > VI$ have occurred since the beginning of the 16th century in southeastern Betics (apart from the last 2011 Lorca earthquake). Eight of these events had a magnitude $M_w > 4.5$ and were located less than 10 km away from the Alhama de Murcia fault trace (Figure 1). Up to now, it has not been identified any geological evidence on the ground surface to associate these events with the activity of specific segments of this fault or any other faults in the area.

Over the last 20 years, several studies have been carried out to analyze the paleoseismic activity and seismotectonic behavior of the most active faults of the Eastern Betics (Carboneras fault, Palomares fault, Alhama de Murcia fault, Los Tollos fault, Carrascoy fault, etc). ([Masana et al., 2004](#); [Silva et al., 2008](#); [Ortuño et al., 2012](#); [Martínez Díaz et al., 2012a](#); [Insua-Arévalo et al., 2015](#); [Martín-Banda et al., 2016](#); [Ferrater et al., 2017](#)) among others (see Quaternary Active Fault Database of Iberia, QAFI v.3, [García-Mayordomo et al., 2015](#)) for a complete references review, see [Data and Resources](#)). In these studies, a number of paleo-earthquakes of magnitudes $M_w > 6.0$ from surface rupturing evidences are identified and dated, some fault activity parameters (average recurrence interval and slip rate) are obtained and different segmentation models of the faults are proposed. Determining which segments were responsible for historical damaging earthquakes $EMS98 > VII$ and/or $M_w > 6.0$ should be a main objective in the analysis of

active faults. Because the date of the last event is a very sensitive parameter in probabilistic seismic hazard calculations, the assignment of these earthquakes to specific faults or segments is of great importance, especially when time-dependent models are considered (e.g., [Mathews et al., 2002](#))

The town of Lorca (Figures 1 and 2) was seriously damaged during the 2011 Mw 5.2 earthquake ([Martínez-Cuevas et al. 2016](#)). Despite its moderate magnitude, this earthquake caused 9 deaths and extensive damage. This city has also suffered another 4 episodes of destruction between the 14th and 19th centuries. In this work we show the results obtained during a paleoseismological exploration of a section of the AMF located 3 km to the SW of Lorca. In the course of this study, we found evidence that support the occurrence of an surface-rupturing earthquake ($M_w > 6.0$) after 1200 AD that we associate with one of the two destructive events that struck the city of Lorca between the 15th and 17th centuries, and most likely with the destructive seismic series that took place in 1674 AD. The excavations carried out in the area of La Torrecilla creek exposed archaeological remains from the Arab period affected by 55 ± 20 cm offset by the AMF fault, as well as other geological evidence of surface deformation. The consideration of this earthquake as the last event of magnitude $M_w > 6.0$ in the Góñar-Lorca segment of the AMF, combined with the local and regional slip rate data available, allows to obtain some conclusions related to the seismic hazard that should be considered in seismic risk analysis in the region.

2 Geological setting

The study area is located in the southwestern section of the Alhama de Murcia Fault (Figure 1). First described by [Montenat \(1973\)](#), the AMF is an 87 km long, N40E-N65E, left-lateral strike-slip fault with reverse component, located in the northeastern part of the Eastern Betics Shear Zone, the Betic segment of the Trans-Alboran Shear Zone ([De Larouziere et al., 1988](#)). In this region the upper crust is made up of basement rocks from the Alpujarride and Maláguide tectonic complexes on which several marine Neogene basins were formed associated with an extensional phase between Burdigalian and Tortonian ages ([Armijo, 1977](#); [Martínez-Martínez and Azañón, 1997](#); [Rodríguez-Fernández et al., 2012](#)). The neotectonic compressional period started at the end of the Neogene linked to the Eurasia and Africa plates convergence. The present-day rate of convergence based on geodetic, geophysical and seismologic data is of the order of 4 to 6 mm/yr directed approximately in the NW direction ([Argus et al., 1989](#); [Fernandes et](#)

al., 2007; Serpelloni et al., 2007). The Eastern Betic Shear system could be absorbing up to 31% of the shortening (Masana et al., 2004). Recent geodetic analysis and strain modelling using local GPS velocity data yielded a horizontal slip rate estimation of 1.5 ± 0.3 mm/yr that includes the Alhama de Murcia Fault (AMF) and the Palomares fault slip rates (Echeverría et al., 2013).

According to the geometry of the fault zone, its geomorphic expression and seismicity rate, Martínez-Díaz et al. (2012a) divided the AMF in four sections (Figure 1): 1) Góñar-Lorca (N40E), characterized by a horse tail termination to the south that merges into a narrow fault zone to the north, the presence of Las Estancias range in the hanging wall and a very low instrumental seismicity rate; 2) Lorca-Totana, where the fault turns into a N60E strike. In this section the deformation is distributed in three branches bounding to the southeast of the La Tercia range and to the NW of the Guadalentín Valley; 3) Totana-Alhama de Murcia (N40E), where the fault has less morphological expression and it also exhibits several strands. One of them turns to a N20E strike bounding the Espuña range, while the other branch continues towards Alhama de Murcia although it is covered by Quaternary deposits; and 4) Alhama de Murcia-Alcantarilla (N45E), where the geomorphic expression of the fault is diffuse, possibly in relation to a transfer of deformation to the Carrascoy fault.

Previous paleosismological studies carried out in two sections of the fault, (Lorca-Totana and Góñar-Lorca) have revealed the occurrence of large earthquakes of magnitude greater than 6.0 and even greater than 7.0, with evidence of surface rupture (Masana et al., 2004, Martínez-Díaz et al., 2012a; Ortuño et al., 2012). Some of these studies identified possible ruptures of historical age but without sufficient dating resolution to be associated with specific earthquakes.

The geological slip rate of the AMF has been calculated in previous works from neotectonic and paleoseismic records with values ranging from 1.6-1.7 mm/yr for the Góñar-Lorca section for the past 200 ka using long-term geological data and offsets of alluvial channels, to 0.8-1.2 mm/yr for the Lorca-Totana section for the past 30 ka using 3D trenching on displaced paleo-channels (Ferrater et al., 2016). These values are consistent with the geodetic estimations (Echeverría et al., 2013).

3 La Torrecilla Site

The area analyzed in this study is located in the northern sector of the Góñar-Lorca section, near the limit with the Lorca-Totana section. In this area the AMF has a complex structure with several compressional strike-slip duplex structures, one of which was responsible for the 2011 Lorca earthquake ([Martínez-Díaz et al., 2012b](#)) (Figures 1 and 2).

We selected the northern sector of the Góñar-Lorca segment to carry out a detailed study of the AMF Holocene activity. Here, the deformation on the fault is concentrated in an unique branch of the AMF in contrast with other segments of the fault where the deformation is distributed among several shear zones. (Figures 1 and 2). In La Torrecilla site the fault separates the metamorphic materials of Las Estancias range on the hanging wall from the Quaternary Guadalentín valley deposits to the southeast. The fault is characterized by a 100 m wide shear zone that flanks the mountain front. This shear zone is composed by Palaeozoic and Triassic units of the Alpujárride and Maláguide complexes that form a 20 m wide band of fault gouge and a band of sheared upper Miocene materials (Figure 2). The Upper Pleistocene alluvial fan deposits located on the southeast edge of the fault zone are tilted and offset by the fault as observed in the detailed field study and the borehole made by [Martínez-Díaz et al. \(2016\)](#).

In order to observe the last events of the AMF, we excavated several trenches at the bottom of La Torrecilla creek, where the fault is covered by very recent fluvial sediments. The excavations exposed these fluvial sediments at the southeast edge of the shear zone that are affected by the last movements of the fault (Figures 3 and 4).

Figure 4 shows a section of the excavation wall in which the trace of the fault appears affecting the Quaternary deposits (units 2 to 9). In the lower part of the trench wall, hard layers of older Quaternary alluvial fan gravel (unit 9) are faulted. Overlaying these gravels there are yellow alluvial silt layers (unit 4) excavated by a paleo-channel filled with fluvial gravels from the creek (unit 2). These gravel layers and the erosive base of the channel are tilted and bended in a similar way as the layers of unit 4 drawing a gentle asymmetric fold over the fault. Unit 4 is a low energy alluvial deposit located close to the rambla course and it is located close to the riverbank, we interpret it to be associated with a temporary pooling and therefore it had to be deposited as horizontal layers. The geometric concordance of the layers of unit 4 and those filling the fluvial channel (see dashed lines in figure 4), supports a tectonic origin for this geometry. Moreover, in a previous phase of the excavation (Figure 4b) it was clearly observed that a gravel wedge

(unit GW) onlaps onto the escarpment produced by the fold associated with the fault movement. The radiocarbon derived age of the silts (4585-4815 yr cal. BP) confirmed the Holocene age for the deformation.

In the same excavation, we found on both walls the remains of an ancient irrigation ditch from the Arab period, situated at a depth of 1.5 m and at a distance of 2.5 m away from the fault. Before the excavation, nothing was known about the existence of this ditch. The analysis of aerial photographs from 1929 revealed that this area of the creek was covered by 4 to 5 m of fluvial gravel deposits (Figure 3). This implies that, at the beginning of the 20th century, the irrigation ditch was buried under more than 6 m of gravel deposits, which supports an older age. The dating of charcoal fragments found in the mortar of the ditch and organic matter in the silts filling it, allowed us to obtain an age between 975-1155 AD for the mortar and 1189-1273 AD for the filling. The latter age postdates the time of abandonment and fossilization of the ditch (Figure 4). These dates support that this is an irrigation ditch from the Arab period, similar to others found in this area and in nearby creeks that were used to drain shallow waters towards the adjacent crops from the Arab epoch until the 20th century ([Roldán-Cañas and Moreno-Pérez, 2007](#)).

The geometry of the deformation affecting units 2 and 4 is consistent with only one event of deformation post-unit 4 and pre-unit 1. The trench analyzed shows evidence of older paleoseismic events prior to the silt deposits of unit 4 that generate several unconformities and a previous complex fracture geometry that will not be analyzed in this work. The paleo-channel affected by the last movement of the fault (unit 2 in figure 4) overlays the deposits that fill the irrigation ditch; this implies that the last deformation event should have affected the ditch.

The ditch is covered by a disorganized colluvial deposit (unit 3) with fragments of Miocene marls from the riverbank, and by fluvial gravels of unit 2. The age of ACE2 sample (1189-1273 AD) represents the age of the sediments filling the ditch. The ditch was probably abandoned after a flooding event that produced erosion and colluvial deposits along the riverbank. A further fluvial erosion-sedimentation episode deposited unit 2. We have no more information to constrain the time span from unit 2 sedimentation to the deformation. This must have occurred after 1189-1273 AD and before the historic flood deposits of unit 1.

4 Analysis of coseismic deformation

To quantify the fault slip associated with the last deformation event we can use the shape of the fold that affects units 2 and 4, and also the deformation undergone by the Arab ditch. The vertical offset observed on the southwest wall of the excavation affecting the base of unit 4 is 38 ± 10 cm. The uncertainty of this value is high since the northeastern wall does not show the alluvial levels of unit 4, and the river levels of gravel appear in a higher position indicating an inclination towards the rambla valley. This situation prevents us from (using the base of unit 4 as a marker?) estimating a reference surface to calculate the net slip.

The excavation of a trench across the fault in the bottom of the La Torrecilla creek was planned without knowledge about the existence of the ditch. Unfortunately, the trench location coincided with the intersection point between the ditch and the fault (Figure 5), and this resulted in the destruction of a section of 5 m of the ditch close to the fault. Despite this, we made a detailed geometric analysis of the ditch because this type of construction presents a constant slope tendency that can be used as a marker to constrain vertical deformation. Additionally, anomalies in the orientation of the path of the ditch can provide information about horizontal deformation. We made an excavation to exhume 20 m of ditch on each side of the fault in order to carry out a detailed topographic survey using GPS data, total station measurements with an instrumental accuracy < 2 cm, and a drone flight to obtain a high-resolution zenithal view (see figure 5 and 6 and videos in the Online Resources 1 and 2).

Figure 5) shows the geometrical analysis of the exhumed irrigation ditch. The azimuthal view of the ditch shows segments varying in length with slightly different orientation having a mean azimuth of $N108^\circ \pm 8^\circ$, except for the two easternmost ones. We identified sixteen straight segments grouped into two types regarding its length: short-length segments with 179 ± 4 cm, and long-length segments with 229 ± 15 cm (mean value ± 1 standard deviation is given). Such a length distribution is probably associated with the succession of several formwork phases during its construction that explains the gentle changes in orientation. There are also two more segments partially destroyed during the trench excavation with a remaining length of 80 and 55 cm at the western and eastern sides of the fault, respectively. To reconstruct the ditch, we have prolonged both partially destroyed segments (maintaining the direction of the remaining parts) considering both possible lengths of the identified segments. In any case the segments get connected, so a third one is needed. The only geometrically possible combination is that one in which three

short-length segments are considered: the two partially destroyed ones plus a third one connecting them (line between dot markers in inset of figure 5b). This third segment should have a direction of ca. N90° to link to the other two segments located at both sides of the fault, which is out of the range of the orientation of all other segments, implying then that the ditch was left laterally offset by the fault. A strike-slip separation of 53 ± 22 cm can be estimated considering the projection on the mean orientation of the ditch (Figure 6b). The error of ± 22 includes the angular error associated to the variability of the orientation of the exhumed segments plus the error of the measurement of the length of the short segments.

To analyze the vertical deformation, a detailed topographic profile of the survey along the ditch was projected in a N108° vertical plane (figure 5c). A slope of ca. 3‰ has been estimated for the ditch at both walls of the fault (dashed line), giving a vertical separation of 14 ± 3 cm. The slope is estimated along the bottom of the ditch (better preserved from degradation than the banks) considering the total station survey data (more accurate than GPS data). A gentle anticline fold was identified on the upthrown block. This is probably associated with dragging near the fault, and the existence of some internal deformation of the sediments due to shortening. A change of slope has been also identified at the easternmost part of the ditch, although no fault strand or lateral displacement has been clearly observed. In addition, a slight tilting of the ditch walls was observed in the ditch sections located less than 5 m away from the fault, which is consistent with some internal deformation of the deposits close to the fault.

Regarding the observations made on the analysis of the vertical deformation we infer that the band of deformation at both sides of the fault reaches up to 11 m width. This implies that the strike-slip offset calculated above considering the ditch displacement on the fault plane would be larger if the width of the deformation band is considered. A maximum value of 2 m can be roughly estimated. However, the range of orientations of the ditch segments is too broad to take it as a reference marker, preventing us from giving an accurate estimate. We rather prefer to consider the nearfield value for the strike-slip to estimate the net displacement, as a minimum value.

The net displacement (D) and pitch (ϕ) values were calculated by the addition of the horizontal and vertical separation vectors on a fault plane dipping 70° NW, as observed in the fault zone exposed at several outcrops and in other trenches. These values are: $D = 55.7 \pm 20.6$ cm and ϕ : 18°.

The vertical separation observed on the wall of the excavation is higher than the vertical separation calculated from the ditch. We consider two reasons that would explain the difference. The trench wall, where that value was observed is located ~3 m away from the point where the ditch intersects the fault plane. This distance could explain some differences in separation values linked to a possible inclination of this stratigraphic layers of units 2 and 4 westwards. In addition, the mechanical heterogeneity of the deposits could explain lateral variations in the partition between vertical and horizontal components of movement linked with internal deformation and material extrusion. For these reasons we consider the value obtained from the ditch to be more reliable, as it represents a rigid and homogeneous body with a flat base prior to deformation.

5 Interpretation

According to the Spanish Seismic Catalogue, since the 16th century the city of Lorca has been affected by 4 destructive earthquakes with intensity greater than VI (IGN, 2017). Only one (2011 Lorca earthquake) have occurred during the instrumental period. The magnitudes (M_w) assigned to the historical events in the homogenized seismic catalog of the Spanish Seismic Hazard Map Project (IGN-UPM, 2013), following the methodology explained in Cabañas et al. (2015), and from the SHARE European Seismic Catalogue (Stucchi et al. (2013) range from $M_w 4.3 \pm 0.4$ to $M_w 6.0 \pm 0.8$ (Figure 7).

From the trench analysis we found evidences of one surface rupture event younger than the abandonment of the ditch (1189-1273 AD). To be more precise, the identified event is younger than unit 2 which is the result of the second sedimentary event recorded after ditch abandonment. There are only two earthquakes in the seismic catalogs located close to Lorca and large enough to be the cause of the observed rupture: 1579 and 1674 Lorca Earthquakes. The 1674 event is by far the most destructive according to the detailed damage analysis from Muñoz-Clarés et al. (2012). Both the Spanish Seismic Hazard Map catalog (IGN-UPM, 2012) and the SHARE catalog (Stucchi et al. 2013) assign to the 1674 event a larger magnitude M_w (Figure 7).

We could consider the possibility of a completeness gap in the seismic catalogue for the period (1189-1273 AD) – 1579. However, the Spanish seismic catalog includes 4 earthquakes in the Eastern Betics from 1048 to 1406 AD with intensities from VII to IX. We believe that it is unlikely that an event with surface rupture in the study area during that period would not have left any evidence in the historical record.

Assuming the interpretation of a single surface rupture event after the sedimentation of unit 2, we consider that the 1674 earthquake is most likely responsible for the deformation observed. The historical documents that describe the damage resulting from this earthquake are mostly centered in Lorca. So far there are no references of historical documents describing damages in surrounding towns. We must take into account that in the 17th century the closest inhabited centers from the section of the fault studied here were located at 25-28 km away. These villages were Totana, Águilas and Vélez Rubio, which at that time had a low administrative development. It is significant that none of these localities have historical references accounting for the effects of earthquakes prior to the 18th century (IGN 2017). The lack of administrative development in that period could explain the absence of historical record.

Historical documents report that the 1674 earthquake reached an intensity EMS VIII (IGN, 2017) at Lorca, with 25% of the buildings destroyed and at least 30 fatalities (Martínez-Guevara, 1985). Muñoz-Clarés et al. (2012) made a very detailed collection and revision of the damage associated with the earthquake. They conclude that the greatest damage took place in the city's southwestern districts (Figure 7b), where almost two-thirds of the buildings were destroyed, followed by areas on the eastern slope of the Lorca Castle hill. In the northern part of the city, to the north of the Guadalentín river, despite the lower quality of the buildings, the damage registered was much lower, only slightly more than 10% of buildings were affected (Muñoz-Clarés et al. 2012). Although damage distribution is not conclusive due to the difficulty of assessing the degree of vulnerability of buildings at that time, it seems that the greatest destruction was concentrated in the southwestern districts.

Recently, Quirós (2017) devised a damage scenario similar to the 1674 event associated with a 975-yr return period for an earthquake of magnitude Mw 6.5 in the Puerto Lumbreras-Lorca section of the AMF using current vulnerability data from the city of Lorca. This model was calibrated with a previous model of damage generated by the 2011 Mw 5.2 earthquake. The 1674-like scenario resulted in an intensity EMS VIII event with 345 fatalities out of a current population of 58,800 inhabitant (0.58 % of population).

According to the data analyzed in [Muñoz-Clarés \(2012\)](#), the 1674 earthquake produced 30 fatalities out of an estimated population of 7300 inhabitants (0.41 % of population). Assuming the difficulty of comparing this type of effects between periods so far apart in time, we think that assigning a magnitude $M_w > 6.0$ for the 1674 event is consistent with the known effects.

To understand the relative size of the 1674 earthquake it is also interesting to compare the characteristics of its aftershock sequence with the 2011 Lorca series that was caused by the rupture of a section of about 3 km long located to the northeast of Lorca ([Martínez-Díaz et al., 2012b](#)) (Figure 7). The 2011 series began with a foreshock of $M_w 4.5$ followed by 6 aftershocks with magnitudes between 1.3 and 2.6. The mainshock of $M_w 5.2$ occurred one hour and 45 minutes later, followed by 135 aftershocks during the next 2 months ([IGN, 2011](#)). Despite the shallow depth of this sequence (< 5 km) only 16 aftershocks were felt by the population and they took place during the week following the mainshock. On the other hand, during the 1674 series the seismic sequence started with an intensity VII foreshock prior to the mainshock, which reached intensity VIII. The mainshock was followed by an aftershock sequence with events felt by the population for more than one month, one of them reaching intensity VII ([Martínez-Guevara, 1985](#)). Although the distribution of damage generated in Lorca by the 1674 earthquake is not conclusive to assign a precise geological size, the seismic characteristics of the series point to an earthquake of magnitude clearly larger than the 2011 ($M_w 5.2$) earthquake, consistent with magnitudes assigned in the historical catalogues, 6.0 ± 0.8 (IGN-UPM, 2013) and 5.9 ± 0.41 (SHARE catalogue, Stucchi et al. 2013).

6 Implications to seismic hazard

The evidence of ground surface deformation identified at La Torrecilla creek site supports the occurrence of a surface-rupturing earthquake postdating the deposits covering the Arab irrigation ditch (1189-1273 AD). The geometric analysis of the ditch and the materials deposited on it provide a net slip of 55.7 ± 20.6 cm with a pitch of 18° that is consistent with the strike-slip kinematics with reverse component that has been observed in paleoseismological trenches excavated in other sections of the AMF ([Ortuño et al. 2012](#); [Ferrater et al., 2017](#)), and it also agrees with the focal mechanism of the 2011 Lorca earthquake ([Lopez-Comino et al., 2011](#)).

We assume that the deformation observed in the trench is all coseismic. Although it is not easy to rule out that part of it may be due to after-slip aseismic deformation. Nevertheless, the episodic character of the deformation, and its similarity to other paleoseismic events of Holocene age identified in other sites along this fault ([Ortuño et al. 2012](#); [Ferrater et al., 2017](#)), support this assumption.

We have estimated the magnitudes that three different rupture scenarios would generate in the Góñar-Lorca segment of the AMF considering a fault width of 12-10 km ([Martínez-Díaz et al., 2015](#)). A first scenario (Sc1 in Figure 1), considers the rupture of the entire Góñar-Lorca segment, with a length of 30 km. A second scenario Sc2 a rupture between Puerto Lumbreras, where a splay fault intersect the main fault, and Lorca (15 km long), and finally, a third scenario, Sc3 considering the rupture of a 10 km long section (in this case we reduced the width to 10 km), including the Lorca strike slip duplex and the sector of the La Torrecilla site where the deformation is mostly concentrated in a narrow band (Figure 6). We first calculate the seismic moment (M_o) from [Aki \(1966\)](#):

$$M_o = A\mu D$$

where A is the rupture area, D is the average displacement on the fault, and μ is the shear modulus. For the net displacement we consider the range found in this study (35-75 cm) and for μ 30 GPa. Secondly, we convert to moment magnitude (M_w) using [Kanamori \(1977\)](#):

$$M_w = \frac{2}{3} \log(M_o) - 10.7$$

the obtained values of M_w oscillate between M_w 6.58 for the scenario Sc1 and M_w 5.96 for the scenario Sc3. It should be noted that these values are presumably an underestimation of the magnitude since the value of the displacement measured on the ground surface is lower than the average displacement on the fault plane, and because part of the coseismic slip could have taken place in other fault branches rather than the one analyzed here. Using the empirical relationships recommended in [Stirling et al. \(2013\)](#) for plate boundary regions and for low velocity strike-slip and reverse faults ([Stirling et al., 2008](#); [Wesnousky, 2008](#) and [Yen and Ma, 2011](#)) we obtain for each scenario the following values: Sc1: M_w 6.5-6.9; Sc2: M_w 6.2-6.6 and Sc3: M_w 5.9-6.4. These values, as might be expected, are higher than those obtained with the estimate of M_w from the [Kanamori \(1977\)](#) equation and range from 5.9 to 6.9.

As described in the geological setting, previous work estimated geological slip rates for the AMF ranging from 0.8 to 1.7 mm/yr during the last 200 ka, and geodetic data provided a slip rate of 1.5 mm/yr in a transect crossing both the Alhama de Murcia Fault and the Palomares fault (Figure 1). In this work we use the latest slip rate estimation of 1.0 ± 0.2 mm/yr obtained by [Ferrater et al \(2017\)](#) for the past 30 ka, in order to make calculations of the theoretical recurrence time of a surface-rupturing earthquake in this region, assuming a homogeneous slip-rate in all sections of the AMF.

The average expected repeat time (RI) of earthquakes on a fault described by the maximum magnitude model from [Wesnowsky \(1986\)](#) can be estimated as:

$$RI = M_o^e / \dot{M}_o^g$$

where M_o^e is the seismic moment of the maximum expected event on the fault and \dot{M}_o^g is the geological moment rate as a function of fault slip rate. With this simple approach that assumes a highly organized stress cycle behavior and a fully coupled interface on the fault, we obtain RI values ranging from 1397-3119 yr for Sc1; 589-1762 yr for Sc2; and 338-1522 yr for the scenario Sc3 (see Table 1).

Summarizing, depending on the considered magnitude scenario (from 5.9 to 6.9, according to the empirical relationship used to estimate the M_w) the theoretical recurrence interval can range from a minimum of 338 yr (Sc3) to a maximum of 3119 yr (Sc1).

The spatial distribution of damage, the maximum intensity, and the structure of the AMF lead us to consider that the magnitude of scenario Sc1 (M_w 6.8-6.9) is too large and it is more suitable a rupture close to scenarios Sc3 and Sc2, with magnitudes from 5.9 to 6.4.

Assuming that the last earthquake on the Góñar-Lorca section occurred in 1674 (343 yr ago, that is close to the lower value of the recurrence interval of Sc3) and a slip rate ranging from 0.8 to 1.2 mm/yr, the slip accumulated up to now would be 27.4 to 41.2 cm. These figures are close to the coseismic displacement identified at La Torrecilla site.

The variation in static stress at this site after the 2011 Lorca earthquake is a further observation suggesting that this fault segment is prone to rupture the surface in a near future. The time of occurrence of an earthquake on a fault segment undergoing tectonic loading is controlled both by the stress and frictional properties on that fault and by earthquakes on other faults or segments nearby ([Stein, 1999](#)). For

a fault loaded at a constant background rate, a positive change of Coulomb failure stress produces a time shift (advance) in the seismic cycle equivalent to:

$$\Delta T = \Delta CFS / \tau$$

where ΔT is the time shift, ΔCFS is the Coulomb failure stress change and τ is the long term stressing rate on the fault.

[Martínez Díaz et al. \(2012b\)](#) calculated the static Coulomb stress change induced by the 2011 Mw 5.2 Lorca earthquake on the surrounding sections of the AMF. They conclude that the Góñar–Lorca segment was charged with a stress change that exceeds 1 bar, a value that was shown to be sufficient for the generation of earthquake triggering ([Stein, 1999](#); [Chen et al., 2010](#)). They also modeled the long term stressing rate on the brittle part of the fault assuming a constant displacement on the ductile deep segment of the fault with a slip rate of 0.1-0.6 mm/yr (slightly lower than the value considered here), and they obtained stress changes between 0.001 and 0.005 bar/year. A stress change of 1 bar would represent on the AMF a seismic cycle advance (time shift) longer than 200 to 1000 years of tectonic loading. This time shift represents a significant fraction of the recurrence time scenarios estimated above.

7 Conclusions

We found evidence that support the occurrence of an earthquake with surface rupture ($M_w > 6.0$) after 1200 AD that we associate with one of the destructive historical earthquakes that caused damage to the town of Lorca, probably the destructive seismic series that took place in 1674. The excavations carried out in the area of La Torrecilla creek exposed archaeological remains from the Arab period affected by 55 ± 20 cm offset by the AMF fault. This is the first geological evidence of the catastrophic event occurred in 1674. This event reached intensity VIII and produced 30 fatalities at Lorca for an estimated population of 7300 inhabitants. This supports the occurrence of earthquakes with surface rupture in the historical epoch on the Alhama de Murcia Fault and reinforces the results obtained in the previous paleoseismological works. The 1674 earthquake with $M_w > 6.0$, should be considered in the future seismic hazard analysis as the last major event in the Góñar-Lorca section of the AMF.

The theoretical scenarios of maximum magnitudes and recurrence time obtained by combining this historical event with the AMF slip rate data allow us to conclude that the seismic hazard associated with

maximum magnitude events in this section could be high. In addition, the static Coulomb stress transferred to the Góñar-Lorca section by the 2011 earthquake may have increased the hazard by inducing a cycle advance of several hundreds of years.

The high dependence of recurrence time and, therefore the seismic hazard values, on fault activity parameters is also highlighted. The results presented in this work reinforce the importance of incorporating the fault activity parameters in the calculations of seismic hazard assessments in the region and the need to obtain additional data dealing with the seismic behavior of the studied segment.

References

- Aki, K. (1966). Generation and propagation of G-waves from the Niigata earthquake of June 16, 1964. II. Estimation of earthquake movement, release energy, and stress-strain drop from waves spectrum, *Bulletin of Earthquake Research. Institute*. 44, 23–88.
- Argus, D. F., Gordon, R.G., DeMets, C., & Stein, S. (1989). Closure of the Africa–Eurasia–North American plate motion circuit and tectonics of the Gloria fault. *Journal of Geophysical Research*, 94(B5), 5585–5602, <http://dx.doi.org/10.1029/JB094iB05p05585>.
- Armijo, R. (1977). La zona des failles Lorca-Totana (Cordillères Bétiques, Espagne). Etude tectonique et neotectonique, Thèse IIIème cycle, Univ. Paris VII: 229 p.
- Cabañas L., Rivas-Medina, A., Martínez Solares, J. M., Gaspar-Escribano, J. M., Benito, B. Antón, R. et al. (2015). Relationships Between Mw and Other Earthquake Size Parameters in the Spanish IGN seismic Catalog. *Pure and Applied Geophysics*, 172(9), 2397–2410, <http://dx.doi.org/10.1007/s00024-014-1025-2>.

Chen, K. H., Bürgmann, R., & Nadeau, R.M. (2010). Triggering effect of M4–5 earthquakes on the earthquake cycle of repeating events at Parkfield, California. *Bulletin of the Seismological Society of America*, 100(2), 522-531. <http://dx.doi.org/10.1785/0120080369>.

De Larouzière, F.D., Bolze, J., Bordet, P., Hernández, J., Montenat, C. & Ott d'Estevou, P. (1988). The Betic segment of the lithospheric Trans-Alboran shear zone during the Late Miocene, *Tectonophysics*, 152, 41–52.

Echeverria, A., Khazaradze, G., Asensio, E., Garate, J., Martín-Dávila, J., & Suriñach, E. (2013). Crustal deformation in eastern Betics from CuaTeNeo GPS network. *Tectonophysics*, 608, 600-612.

Fernandes, R.M.S., Miranda, J. M., Meijninger, B. M. L., Bos, M. S., Noomen, R., Bastos, L. et al. (2007). Surface velocity field of the Ibero-Maghrebian segment of the Eurasia–Nubia plate boundary *Geophysical Journal International* 169(1), 315–324. <http://dx.doi.org/10.1111/j.1365-246X.2006.03252.x>.

Ferrater, M., Ortuño, M., Masana, E., Pallas, R., Perea, H., Baize, et al. (2016). Refining seismic parameters in low seismicity areas by 3D trenching: the Alhama de Murcia fault, SE Iberia. *Tectonophysics*, **680**, 122-128. <http://dx.doi.org/10.1016/j.tecto.2016.05.020>.

Ferrater, M., Ortuño, M. Masana, E., Martínez-Díaz, J. J., Pallàs, R., & Perea, H. (2017). Lateral slip rate of Alhama de Murcia fault (SE Iberian Peninsula) based on a morphotectonic analysis: Comparison with paleoseismological data. *Quaternary International*, 451, 87–100; <http://doi.org/10.1016/j.quaint.2017.02.018>.

García-Mayordomo, J. (2005). Caracterización y Análisis de la Peligrosidad Sísmica en el Sureste de España, *Ph.D. thesis*, Universidad Complutense, Madrid, Spain. Universidad Complutense de Madrid, 373 pp.

García-Mayordomo, J., Gaspar-Escribano, J. M., & Benito, B. (2007). Seismic hazard assessment of the Province of Murcia (SE Spain): analysis of source contribution to hazard. *Journal of Seismology*, 11, 453-471.

IGME (2015). QAFI v.3: Quaternary Active Faults Database of Iberia. Last accessed November 4, 2017, from IGME web site: <http://info.igme.es/QAFI>

Instituto Geográfico Nacional, IGN (2011). Informe del sismo de Lorca 2011 NE Lorca (Murcia), Madrid. <http://www.ign.es/web/resources/sismologia/> (last accessed October 2017)

Instituto Geográfico Nacional, IGN (2017). The Spanish seismic catalogue. IGN-Instituto Geográfico Nacional. Catálogo Sísmico Nacional <http://www.ign.es>. Last accessed November 4, 2017.

IGN-UPM (2013). Actualización de mapas de peligrosidad sísmica de España. 2012. Instituto Geográfico Nacional, 267 pp. ISBN-978-84-416-2685-0.

Insua-Arévalo, J.M., García-Mayordomo, J., Salazar, A., Rodríguez-Escudero, E., Martín-Banda, R., Álvarez-Gómez, J. A. et al. (2015). Paleoseismological evidence of Holocene activity of the Los Tollos Fault (Murcia, SE Spain): A lately formed Quaternary tectonic feature of the Eastern Betic Shear Zone. *Journal of Iberian Geology*, 41(3), 333–350, http://dx.doi.org/10.5209/rev_JIGE.2015.v41.n3.49948.

Kanamori, H. (1977). The energy release in great earthquakes. *Journal Geophysical Research*, 82, 2981–2987. <http://dx.doi.org/10.1029/JB082i020p02981>.

Lopez-Comino, J.A., Mancilla, F., Morales, J., & Stich, D. (2012). Rupture directivity of the 2011, Mw 5.2 Lorca earthquake (Spain). *Geophysical Research Letters*, 39, L03301, <http://dx.doi.org/10.1029/2011GL050498>.

Martín-Banda, R., García-Mayordomo, J., Insua-Arévalo, J. M., Salazar, A., Álvarez-Gómez, J. A., Rodríguez-Escudero, E., et al. (2016). New insights on the seismogenic potential of the Eastern Betic Shear Zone (SE Iberia): Quaternary activity and paleoseismicity of the SW segment of the Carrascoy Fault Zone. *Tectonics*, 35, 55–75, <http://dx.doi.org/10.1002/2015TC003997>.

Martínez-Cuevas, S. & Gaspar-Escribano, J. (2016). Reassessment of intensity estimates from vulnerability and damage distributions: the 2011 Lorca earthquake. *Bulletin of Earthquake Engineering*, 14, 2679-2703.

Martínez-Díaz, J.J., Masana, E., Hernández-Enrile, J. L., & Santanach, P. (2001). Evidence for coseismic events of recurrent prehistoric deformation along the Alhama de Murcia fault, southeastern Spain. *Acta Geologica Hispanica*, 36(3-4), 315–327.

Martínez-Díaz, J.J., Masana, E. & Ortuño, M. (2012a). Active tectonics of the Alhama de Murcia fault, Betic Cordillera, Spain. *Journal of Iberian Geology* 38, 269–286, http://dx.doi.org/10.5209/rev_JIGE.2012.v38.n1.39218.

Martínez-Díaz, J.J., Béjar-Pizarro, M., Álvarez-Gómez, J. A., Mancilla, F. L., Stich, D., Herrera, G., & Morales, J. (2012b). Tectonic and seismic implications of an intersegment rupture. *Tectonophysics*, **546-547**, 28-36, <http://dx.doi.org/10.1016/j.tecto.2012.04.010>.

Martínez-Díaz, J.J., Ortuño-Candela, M., Masana, E., & García-Mayordomo J. (2015). Alhama de Murcia Fault: Góñar-Lorca segment (ES626). In: *Quaternary Active Faults Database of Iberia* v.3.0 - November 2015 (García-Mayordomo et al., eds.), IGME, Madrid. <http://info.igme.es/QAFI>.

Martínez-Díaz, J.J., Insua-Arévalo, J.M., Tsige, M., Rodríguez-Escudero, E., Alonso-Henar, J. Crespo, J. et al. (2016). FAM-1 Borehole: first results from the scientific drilling of the Alhama de Murcia Fault, Betic Cordillera, Spain, *GeoTemas* 16(2), 579-582.

Martínez-Guevara, J. B. (1985). Sismicidad histórica de la Región de Murcia. IX Coloquio de Geógrafos Españoles. A.G.E. Univ. de Murcia. 10 pp.

Martínez-Martínez, J.M., & Azañón J.M. (1997). Mode of extensional tectonics in the southeastern Betics (SE Spain): implications for the tectonic evolution of the peri-Alborán orogenic system. *Tectonics*, 16, 205–225. <http://dx.doi.org/10.1029/97TC0015>.

Masana, E., Martínez-Díaz, J. J., Hernández-Enrile, J. L., & Santanach, P. (2004). The Alhama de Murcia fault (SE Spain), a seismogenic fault in a diffuse plate boundary: Seismotectonic implications for the Ibero-Magrebien region. *Journal of Geophysical Research*. 109(B1), 1–17, <http://dx.doi.org/10.1029/2002JB002359>.

Mathews M.V., Ellsworth, W. L., & Reasenber, P.A. (2002). A Brownian model for recurrent earthquakes. *Bulletin of the Seismological Society of America*, 92(6), 2233–2250, <http://dx.doi.org/10.1785/0120010267>.

Muñoz-Clarés, M., Fernández-Carrascosa, M., Alcolea-López, M. O., Arcas-Navarro, M. C., Arcas-Ruiz, N., Caro del Vas, P., Cruz López, M. T., García Poveda, M., García Valera, M. A., Llamas Martínez B. and Ruiz Llanes A. E. (2012). Sismicidad histórica y documentación municipal: el caso de Lorca. *Boletín Geológico y Minero*, 123(4), 415-429.

Montenat, C. (1973). Les Formations Néogènes du Levant Espagnol. *Ph.D. thesis*, Orsay, France, University of Paris, 1170 p.

Ortuño, M., Masana, E. García-Meléndez, E, Martínez-Díaz, J. J., Stepancikova, P., Cunha, P., et al. (2012). An exceptionally long paleoseismic record of a slow-moving fault: the Alhama de Murcia fault (Eastern Betic Shear Zone, Spain). *Geological Society of American Bulletin*, 124(9-10), 1474-1494. <http://dx.doi.org/10.1130/B30558.1>.

Quirós, L. (2017). Modelizaciones y análisis de sensibilidad en la evaluación del riesgo sísmico a escala urbana. Aplicación a la ciudad de Lorca (in spanish), *Ph.D. thesis*, Universidad Politécnica de Madrid, Madrid, Spain, 399 p.

Roldán-Cañas, J., & Moreno-Pérez, M.F. (2007). La ingeniería y la gestión del agua de riego en Al-Andalus, *Ingeniería del Agua*, 14, 223-236.

Rodríguez-Escudero, E., Martínez-Díaz, J. J., Álvarez-Gómez, J.A., Insua-Arévalo, J.M., & Capote, R. (2014). Tectonic setting of the recent damaging seismic series in the Southeastern Betic Cordillera, Spain. *Bulletin of Earthquake Engineering*, 12(5), 1831–1854, <http://doi.10.1007/s10518-013-9551-3>

Rodríguez-Fernández, J., Azor, A., & Azañón, J.M. (2012). The Betic intramontane basins (SE Spain): stratigraphy, subsidence, and tectonic history. In: Busby, C., Azor, A. (Eds.), *Tectonics of Sedimentary Basins: Recent Advances*, 23. Blackwell Publishing Ltd, pp. 461-479.

Serpelloni, E., Vannucci, G., Pondrelli, S., Argnani, A., Casula, G., Anzidei, M. et al. (2007). Kinematics of the western Africa-Eurasia plate boundary from focal mechanisms and GPS data, *Geophysical Journal International*, 169(3), 1180-1200. <https://doi.org/10.1111/j.1365-246X.2007.03367.x>.

Silva, P.G., Bardají, T., Calmel-Avila, M., Goy, J. L., & Zazo C. (2008). Transition from alluvial to fluvial systems in the Guadalentín depression (SE Spain) during the Holocene: Lorca fan versus Guadalentín river. *Geomorphology*, 100(1-2), 140-153.

Stein, R. S. (1999). The role of stress transfer in earthquake occurrence. *Nature*, 402, 605–609.

Stirling, M.W., Goned, T., Berryman, K. R., & Litchfield, N.J. (2013). Selection of earthquake scaling relationships for seismic hazard analysis. *Bulletin of the Seismological Society of America*, 103(6), 2993-3011, <https://doi.org/10.1785/0120130052>.

Stirling, M. W., Gerstenberger, M. C., Litchfield, N. J., McVerry, G. H., Smith, W. D., Pettinga, J. et al. (2008). Seismic hazard of the Canterbury region, New Zealand: New earthquake source model and methodology. *Bulletin of the New Zealand Society for Earthquake Engineering*, 41, 51–67.

Stucchi, M., Rovida, A., Gomez Capera, A. A., Alexandre, P., Camelbeeck, T., Demircioglu, M.B., Gasperini, P., Kouskouna, V., Musson, R.M.W., Radulian, M., Sesetyan, K., Vilanova, S., Baumont, D., Bungum, H., Fäh, D., Lenhardt, W., Makropoulos, K., Martinez Solares, J. M., Scotti O., Živčić, M., Albini, P., Batllo, J., Papaioannou, C., Tatevossian, R., Locati, M., Meletti, C., Viganò, D., and Giardini D. (2013). The SHARE European Earthquake Catalogue (SHEEC) 1000-1899. *Journal of Seismology*, 17, 2, pp.524-544. doi: <http://doi.org/10.1007/s10950-012-9335-2>

Wesnousky, S.G. (1986). Earthquakes, Quaternary faults, and seismic hazard in California. *Journal of Geophysical Research*, 91(B12), 12587-12631.

Wesnousky, S. G. (2008). Displacement and geometrical characteristics of earthquake surface ruptures: Issues and implications for seismic-hazard analysis and the process of earthquake rupture. *Bulletin of the Seismological Society of America*, 98, 1609–1632.

Yen, Y.T., & Ma, K. F. (2011). Source-scaling relationship for M 4.6–8.1 earthquakes, specifically for earthquakes in the collision zone of Taiwan. *Bulletin of the Seismological Society of America*, 101, 464–481.

Table Caption

Table 1 Parameters of the three scenarios discussed. The M_w is calculated as the average of the values obtained from the empirical relationships recommended in [Stirling et al., \(2013\)](#) for slow plate boundary and stable continental faults ([Stirling et al., 2008](#) (for oblique slip faults); [Wesnousky, 2008](#); [Yen and Ma, 2011](#); [Anderson, 1996](#)). RI-ME is the recurrence interval calculated considering the maximum earthquake model of [Wesnousky \(1986\)](#) and the slip-rate range considered.

Figure Captions

Fig 1. Map showing the location of the Alhama de Murcia fault (AMF) in the eastern sector of the Trans-Alboran Shear Zone (TASZ). The fault line of the AMF that limits the Neogene basins and ranges located to the NW of the Quaternary Guadalentín Valley to the southeast and the other active faults in the region are plotted on the digital elevation model (CRF: Crevillente fault; CF: Carrascoy fault; PF: Palomares fault). The epicenters of instrumental seismicity with magnitude $M_w > 3.0$ and the historical seismicity of intensity (EMS98) $> V$ are also plotted, data from [IGN \(2017\)](#). The square indicates the situation of the detailed geological map of figure 2, and the white star shows the position of La Torrecilla site where surface rupture evidence is analyzed. Arrows show the GNSS velocity vectors from [Echeverria et al. \(2013\)](#) referred to Eurasian plate, together with the regional African-Eurasian plates convergence (5 - 6 mm/yr). The three rupture scenarios (Sc1-3) analyzed in the text are marked with dashed lines.

Fig. 2. Geological map of the northeast sector of the Góñar-Lorca segment of the Alhama de Murcia fault (AMF). The AMF shear zone is more than 100 m wide and it is characterized by a well-developed fault gouge of paleozoic and mesozoic rocks from the Maláguide and Alpujárride complexes (black band), as well as slivers and bands of Miocene materials included in the shear deformation zone. Quaternary materials formed by Pleistocene and Holocene alluvial fans, and Holocene rambla deposits are deformed

at some points. The fault lines mark the limits of the sheared fault zone, that is highlighted with a pattern of parallel lines. The position of the excavation trench in the bottom of the La Torrecilla creek is indicated by a rectangle. The prolongation towards the NE of the fault trace identified in the creek is inferred from old aerial photographs (see explanation in text) and it is consistent with the SE edge of the strike slip duplex on top of which the city of Lorca is located (see figure 5).

Fig. 3. A: Aerial photographs taken in 1929 and 2011 of the La Torrecilla site. The oldest photo clearly shows the layer of fluvial gravel that filled the riverbed of the rambla in the recent past. B: Oblique aerial view (from the south) of the excavated ditch (see Figure S2). C: A detail of the ditch and the limes filling it.

Fig. 4. a) Photograph of the SW wall of the paleosismological excavation carried out in the course of the Torrecilla creek (see location in figure 2). b) Photograph of the first phase of the excavation where a fold was observed affecting Holocene limes (unit 4) with a gravel wedge on lapping the scarp (GW). In the hanging wall, an ancient irrigation ditch from the Arab period was observed (see age in c)) excavated on materials deformed by the fault activity and covered by gravel deposits (unit 2), which are also involved in the deformation. Sedimentary units: 1: Very recent fluvial gravel from the creek (human remains found indicate 20th century age); 2: Creek fluvial gravel; 3: Irrigation ditch (a) covered by a disorganized clay colluvium with clasts; 4: Lime and sand (dated in 4.5-4.8 ka); 5: Colluvial deposit formed by clasts of metamorphic rocks and silts. 6 and 7: Creek fluvial gravel showing different degree of deformation. 8: Colluvial deposits with fragments of Miocene silts and conglomerates coming from the creek banks. 9: Cemented gravel of Pleistocene alluvial fan.

Fig. 5. Geometrical analysis of the deformed ditch. a) Aerial photo of the exhumed irrigation ditch. The position of previous paleoseismological trench analyzed in figure 5 is labelled. b) Plan view of the topographic survey performed along the ditch: total station and differential-GPS measurements. The inset shows the analysis of the length and orientation of ditch segments. A strike-slip separation of 53 ± 22 cm has been estimated (see text for interpretation). c) Topographic profile of the surveyed points along the ditch projected in a $N108^\circ$ vertical plane. A slope of ca. 3‰ has been estimated for the ditch at both sides

of the fault (dashed line). The slope is fitted along the ditch bottom (which is better preserved from degradation than the banks). A slight anticline has been identified on the upthrown block probably related to fault displacement. A change of slope has been also identified at the easternmost part of the ditch, although no fault strand or displacement has been observed.

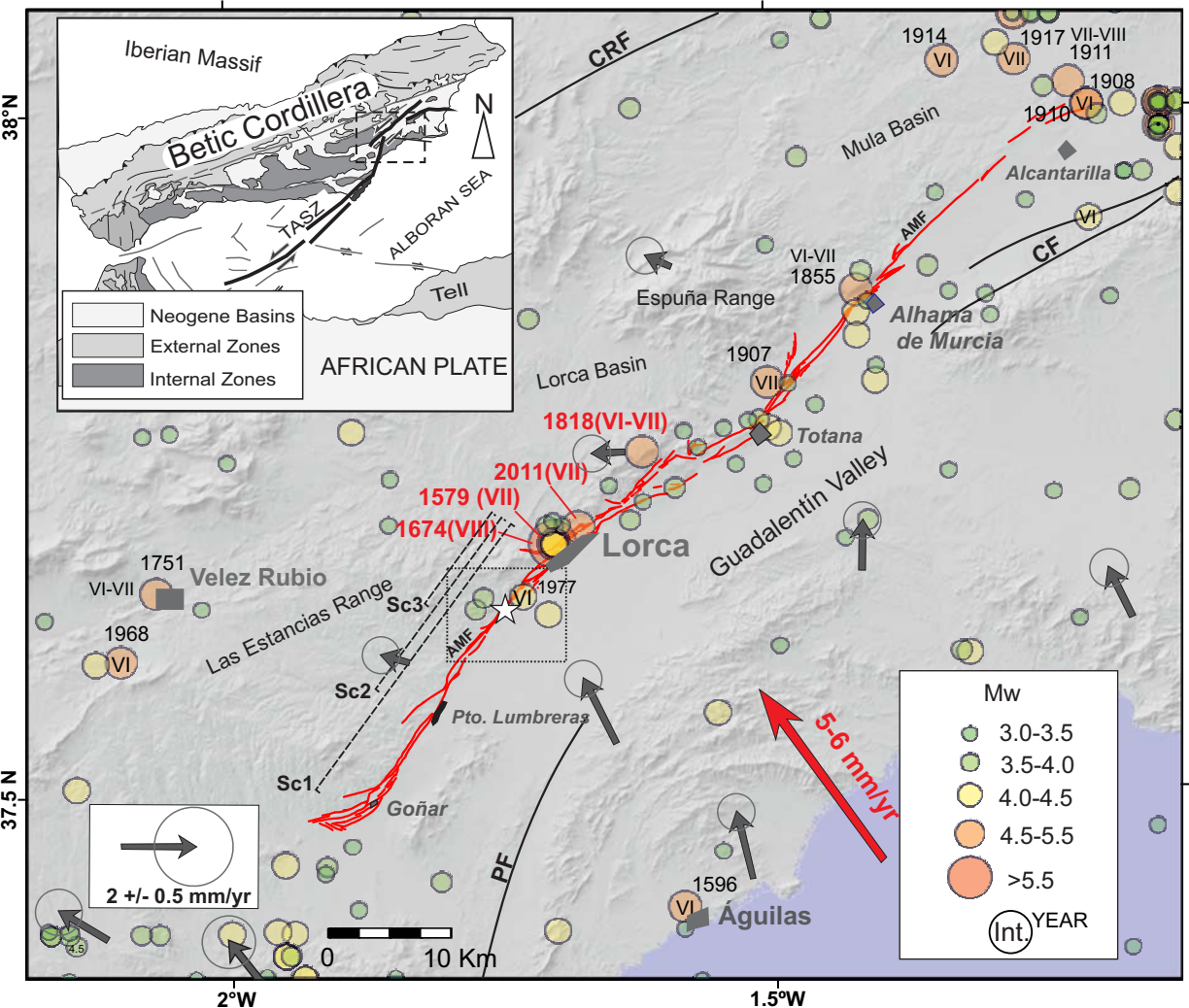
Fig. 6. A: Oblique view (from the East) of the exposed irrigation ditch. White line indicates the position of the previous paleoseismological trench, the orange rectangle marks the wall section shown in figure 5. The red line is the fault trace and the yellow line indicates the section where the ditch walls are tilted to the west. B and C show a profile view and an oblique view of the 3d spatial analysis of the modelled ditch, carried out to identify and quantify deformations shown in figure 4.

Fig. 7. A: Map of the local structure of the AMF in the vicinity of Lorca. In this sector, the AMF structure is characterized by the presence of two "contractional strike slip duplex" Matalauva strike slip duplex (MSSD) and Lorca strike slip duplex (LSSD). The map view projection of the rupture responsible for the 2011 Mw 5.2 destructive Lorca earthquake (according to Martínez-Díaz et al. 2012) is marked with the dashed square. The star shows the position of the surface rupture observed at La Torrecilla Site. The dark arrowed line shows one of the possible rupture scenarios proposed in this work (Sc3) that would imply the reactivation of the fault bounding the LSSD. The triangles are the epicenters of the historical earthquakes of intensity > V according to the Spanish Seismic Catalogue (IGN) b: Distribution of damages generated by the catastrophic earthquake of 1674 in the parishes of Lorca according to (Muñoz-Clarés, 2012). Darker grey areas indicate the parishes with the highest degree of destruction (zone 1), light grey (zone 3) indicates the less affected areas and zone 2 indicates those areas with an intermediate degree of damage. The table shows the parameters of the damaging earthquakes recorded in Lorca since 16th century, taken from the Spanish Seismic Catalogue of Instituto Geográfico Nacional (IGN, 2017). Magnitudes (Mw1) are from the catalogue of the Spanish Seismic Hazard Map project" (IGN-UPM, 2013), following the methodology explained in Cabañas et al. (2015) and Mw2 from the SHARE European Earthquake Catalogue (Stucchi et al. 2013).








Electronic supplementary material

Resource 1: Video from aerial views taken with drone flying over the exhumed ditch. The excavation oblique to the ditch is the previous excavation dug to look for the fault plane rupture that unfortunately destroyed the section of the ditch in contact with the fault. The flight trajectory goes from north to south.

Resource 2: Video from aerial views taken with drone flying over the exhumed ditch. The flight trajectory goes from south to north.



4167000

Neotectonic MaterialsQuaternary  Alluvial fan deposits and fluvial sedimentsMiocene  Yellow marls interbedded with sandstones
 Orange sand and clayey sand and conglomerates**Maláguide Complex**Permian-Triassic  Wine-red phyllites and quartzites**Alpujarride Complex**Permian-Triassic  Yellow, green and brown quartzites and phyllites
 Blue-gray Phyllites and schists and quartzitesPaleozoic  Graphitic mica-schists and quartz-schists AMF shear deformation zone

4166000

4165000

